TITLE PAGE

In Ovo Sexing of Chickens through VOCs: Assessment of System, Setup, and Day-to-Day Performance using HSSE-GC-MS, PTR-TOF-MS, and SIFT-MS

Matthias Corion[a,b], Miguel Portillo-Estrada[c], Simão Santos[a], Nadia Everaert[b], Jeroen Lammertyn[a], Maarten Hertog[d], Bart De Ketelaere[e,1]

[a] KU Leuven, MeBioS Biosensors group, Department of Biosystems, Leuven, Belgium

[b] KU Leuven, A2H Nutrition & Animal EcoSystems (NAMES) Lab, Department of Biosystems, Leuven, Belgium

[c] University of Antwerp, Research Group Pleco, Department of Biology, Wilrijk, Belgium

[d] KU Leuven, MeBioS Postharvest group, Department of Biosystems, Leuven, Belgium

[e] KU Leuven, MeBioS Biostatistics group, Department of Biosystems, Leuven, Belgium

[1] Corresponding author: E-mail: bart.deketelaere@kuleuven.be Telephone: +32 16 32 85 93

ABSTRACT

In ovo sexing involves identifying chicken embryo sex before or during incubation to avoid euthanizing male chicks after hatching, enhancing animal welfare in the laying hen industry. Recently, researchers demonstrated the potential for non-invasive and early in ovo sexing through the analysis of volatile organic compounds (VOCs) emitted by eggs. However, a knowledge gap persists in comprehending the robustness of prediction models, the efficacy of faster acquisition techniques, and the day-to-day performance variations. In our study, we performed two experiments to fill these gaps. In Experiment 1, passive VOC extractions were performed on 110 eggs on incubation day 10 using sampling bags employing headspace sorptive extraction-gas chromatography-mass spectrometry (HSSE-GC-MS), proton transfer reaction-time-of-flight-mass spectrometry (PTR-TOF-MS), and selected ion flow tube-mass spectrometry (SIFT-MS). Prediction models were built using partial least squares-discriminant analysis (PLS-DA) and variable selection methods. As a result, prediction accuracies ranged from 57.6 % to 61.4 %, indicating no significant difference between the devices and highlighting the need for further optimizations. In Experiment 2, passive VOC samplings were performed on 42 eggs in glass jars during the initial 12 days of incubation using HSSE-GC-MS. Consequently, the optimized setup yielded higher accuracies ranging from 63.1 % to 71.4 %, revealing VOCs consistently elevated in relative abundance for a specific sex, and overall VOC abundance was higher in male embryos. Suggestions for future experiments to increase the accuracy of VOC in ovo sexing include active sampling with inert materials, expanding sample sets, and targeting consistent compounds.

KEYWORDS

In ovo sexing, Animal welfare, Chicken eggs, Male day-old culling, Volatile Organic Compounds (VOCs), Mass spectrometry

NOMENCLATURE

FEP	Fluorinated Ethylene Propylene
FiPLS	Forward interval partial least squares
GC-MS	Gas chromatography-mass spectrometry
HSSE	Headspace sorptive extraction
HSSE-GC-MS	Headspace sportive extraction-gas chromatography-mass spectrometry
JK	Jackknifing
PLS-DA	Partial least squares-discriminant analysis
PTR-TOF-MS	Proton transfer reaction-time-of-flight-mass spectrometry
SIFT-MS	Selected ion flow tube-mass spectrometry
SPME	Solid phase microextraction
VIP	Variable importance in projection
VOC	Volatile organic compound

1. Introduction

In the laying hen industry, culling one-day-old male chicks is currently a standard procedure (Bruijnis et al., 2015). Annually, approximately 7 billion male chicks are culled worldwide right after hatch (Krautwald-Junghanns et al., 2018). This practice originates from the economic devaluation of layer roosters, attributable to their inefficient growth for meat production in contrast to broiler chickens (Giersberg and Kemper, 2018). Recently, Germany (Bundestag, 2019), France (République Française, 2022), and Italy (Governo Italiano, 2023) have enacted legislation that prohibits these culling practices. On the one hand, this legislation mandates sexual determination, in ovo sexing, and egg separation before the potential onset of embryo pain perception, which was recently defined after 13 days when physiological neuronal signals could be determined (Kollmansperger et al., 2023). On the other hand, if not culled before pain perception, male chickens have to be reared. However, this last option results in a higher environmental impact and is predominantly tailored to niche market demands since most consumers do not appreciate the product (Busse et al., 2019).

Thus, in ovo sexing is preferred by the industry to resolve the male day-old chick culling issue since it avoids investing in male chickens and allows embryo disposal before pain perception (Reithmayer et al., 2021). Numerous researchers and institutions have been developing in ovo sexing technologies. Through a comprehensive analysis in an earlier study of 49 scientific papers and 115 patents, we have defined 11 different in ovo sexing techniques and categorized them into five optical and six non-optical methods (Corion et al., 2023b). In Europe, there are currently two commercially available optical techniques. One employs magnetic resonance imaging to assess gonad asymmetries on day 12 (Haase et al., 2019), while the other utilizes visible-near infrared light absorption for color sexing on day 13 (McKay, 2014). A key advantage of both techniques is

their non-invasive nature, mitigating the risks associated with contamination. A challenge encountered with magnetic resonance imaging pertains to the ongoing validation of prediction accuracies, which must demonstrate robustness to achieve the desired sexing accuracy of up to 98 % (Corion et al., 2023b). Concerning color sexing, this method is only applicable to brown egg-laying breeds exhibiting sex-specific feather coloring after 13 days of incubation, coinciding with the onset of pain perception (Corion et al., 2022).

Furthermore, three commercially available non-optical techniques are applicable as early as day 9 of incubation and involve the analysis of allantoic fluid extracted from the egg. These techniques focus on biomarkers such as metabolites (Bruins and Stutterheim, 2017), hormones (Einspanier, 2017), or DNA (Weigel et al., 2017). The approach utilizing metabolites permits quicker analysis, albeit with the lowest prediction accuracy among the three approaches, surpassing 95 % (Drouin et al., 2023). Higher prediction accuracies of 97 % and 99 % are obtained with the hormone and DNA analysis approaches, respectively. However, both approaches require reagents and have assay incubation times of around 30 to 45 minutes (Corion et al., 2023b). While these non-optical techniques can be applied earlier than the presently commercialized methods, they necessitate fluid extraction and are therefore considered invasive.

In recent years, researchers started studying volatile organic compounds (VOCs) emitted from the eggs of quails (Webster et al., 2015), swallows (Costanzo et al., 2016), and chickens (Xiang et al., 2022; Borras et al., 2023), examining their potential correlation with the sex of the developing embryos. This investigation revealed that VOC in ovo sexing holds the capability to non-invasively assess these compounds released from the egg, even already at the start of the incubation (Xiang et al., 2022). In a standard procedure, eggs are placed within a container to accumulate a headspace. After a defined incubation period, VOC extraction is executed passively by exposing

the equilibrated headspace to a sorbent such as a solid-phase microextraction (SPME) fiber (Webster et al., 2015) or a Twister® stir bar for headspace sorptive extraction (HSSE; Borras et al., 2023), or by conducting a direct headspace analysis (Rivers, 2021). In contrast to passive sampling, researchers have demonstrated the feasibility of actively sampling VOCs from the eggs using suction cups (Borras et al., 2023). Compared to the relatively slow gas chromatography-mass spectrometry (GC-MS), the patent literature outlines faster acquisition methods for measuring egg VOCs. These include chemical ionization techniques such as proton transfer reaction-time-of-flight-mass spectrometry (PTR-TOF-MS) and selected ion flow tube-mass spectrometry (SIFT-MS) (Rivers, 2021), along with optical methods such as Terahertz spectroscopy (Knepper et al., 2018; Gabbai, 2019; Tongli et al., 2019). Both active sampling and new measurement techniques are bringing VOC in ovo sexing closer to commercial implementation.

Although the studies discovered significant differences in VOCs between males and females, only one study constructed classification models to predict the embryo's sex (Borras et al., 2023). In this study, the reported prediction accuracies were constrained to approximately 77 % on days 8, 9, and 10, indicating a need for improvement. Furthermore, there remains a gap in our understanding regarding the robustness of these models and the reproducibility of their accuracies. This knowledge gap is intrinsically linked to the restricted dataset sizes, stemming from the conventional GC-MS analysis which takes tens of minutes to one hour. The adoption of faster acquisition techniques is anticipated to allow for more data and faster analysis times (in terms of seconds), which is also crucial for commercial implementation (Corion et al., 2023b).

In our study, we aim to assess the viability of VOC in ovo sexing using three different analytical systems: headspace sorptive extraction-gas chromatography-mass spectrometry (HSSE-GC-MS) and the faster acquisition techniques PTR-TOF-MS and SIFT-MS. Therefore, a large set of around

100 eggs were incubated and their VOC profiles were measured on day 10 using these three techniques. Additionally, a second experiment was conducted on a smaller set of 42 eggs on the GC-MS. There, the aim was to evaluate sex prediction performance and identify relevant VOCs during the initial days of incubation, before the onset of pain perception, specifically on days 0, 2, 4, 6, 8, 10, and 12. These findings offer valuable insights into the feasibility of predicting embryo sex using VOCs, employing different devices, at different days of incubation.

2. Materials and methods

2.1. Egg Samples

Two separate experiments were carried out to collect VOCs from eggs using different analytical systems. All hatching eggs were purchased from Hatchery Verhaege – Het Anker (Wervik, Belgium). **Table 1** provides an overview of the three different batches of *Isa Brown* eggs originating from three different flocks, along with their usage per experiment. The eggs were not older than 5 days before incubation started and they were stored at 18 °C and minimally 60 % relative humidity. The eggs were incubated under standard conditions (37.7 °C and 55 % relative humidity) in an RCOM Maru 380 max (Autoelex Co. Ltd., Deokam-ri, Republic of Korea). During the process, they were tilted every hour. On day 14, the eggs were removed from the incubator to visually assess fertility and day of death with breakout analysis, following the guidelines from the hatchery practice manual of Aviagen (Huntsville, AL; Tullett, 2009). After the breakout, living embryos were decapitated with sharp scissors, and the sex was determined through feather sexing and gonad assessment. The performed experiment was approved by the Animal Ethics Committee of the KU Leuven under project number ECD P025/2019.

Table 1 – Overview of the *Isa Brown* eggs used in Experiments 1 and 2.

	Batch 1	**Batch 2**	**Batch 3**
Experiment	1	1	2
Analytical device	HSSE-GC-MS & PTR-TOF-MS	SIFT-MS	HSSE-GC-MS
Age of flock	57 weeks	54 weeks	65 weeks
Number of eggs	110	110	42

2.2. Headspace incubation and extraction

Fig. 1 illustrates the two experiments. In Experiment 1, 110 eggs on day 10 were measured in 125 mm by 170 mm fluorinated ethylene propylene (FEP) bags with polypropylene valves (Sense Trading, Groningen, Netherlands) using HSSE-GC-MS, PTR-TOF-MS, and SIFT-MS. After placing an egg in a bag, the bag was closed with a slide-on bag sealer. In Experiment 2, 42 eggs were measured on days 0, 2, 4, 6, 8, 10, and 12 in custom-made glass jars with an average volume of 135 mL using HSSE-GC-MS. After an egg was positioned in a bag or a jar, eggs were individually incubated together with a 10 mm long sorbent stir bar with 1 mm polydimethylsiloxane (PDMS) coating (Twister®, Gerstel, Mülheim an der Ruhr, Germany) that was placed on a stainless steel grid next to the egg. The incubation took place at 37.7 °C for 2 hours to allow for headspace accumulation. After accumulation, the bags' headspace was analyzed using PTR-TOF-MS and SIFT-MS, while the Twisters® from both bags and jars were later subjected to analysis using HSSE-GC-MS. During the measurement sessions, one to three blank measurements were conducted per day as a reference for background compounds. The blank measurements followed the same protocol but without the presence of an egg.

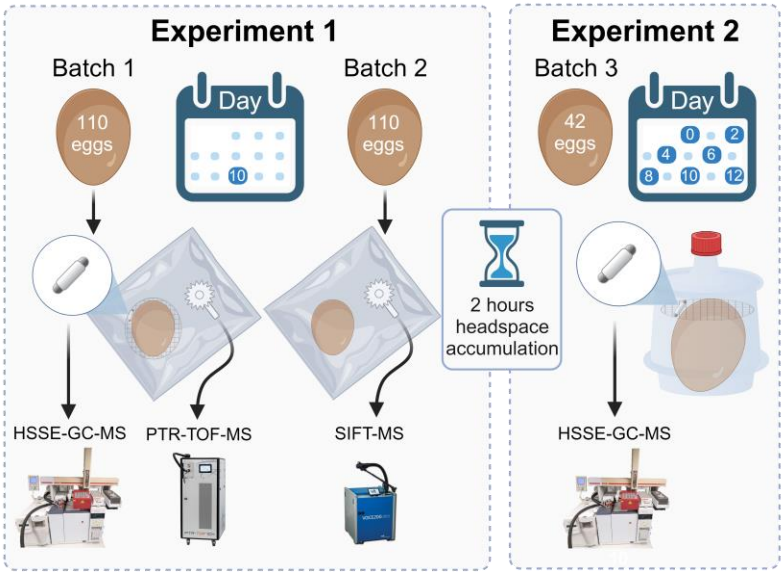

Fig. 1 – Visual representation of the measurement setups for Experiments 1 and 2. Eggs from Batches 1 and 2 were employed in Experiment 2, while those from Batch 3 were used in Experiment 2. Experiment 1 employed FEP bags, whereas headspace accumulation in Experiment 2 was conducted using glass jars (figure made with BioRender.com).

2.3. Recipient flushing, filling, and cleaning

Concerning bag flushing and filling, a 100 mL SGE analytical gas-tight syringe (Trajan Scientific and Medical, Ringwood, Australia) equipped with stainless steel Luer-lock valves and Polytetrafluorethylene tubing and connectors, was used to draw air in and out of the bag. The inlet air was filtered through a Supelcarb hydrocarbon trap (Supelco, Bellefonte, PA) while the outlet air was exhausted into the room. The bags were flushed twice before they were finally filled up to 300 mL for headspace accumulation. Following each bag measurement, they underwent a thermal cleaning process wherein they were automatically flushed with hot air at 100 °C three times using a thermal heat purger (Model SP20, Scentroid, Whitchurch-Stouffville, Canada). For Experiment 2, the jars with eggs were flushed with pressurized air filtered through a Donaldson® hydrocarbon filter (DF-T0050-ZK, Donaldson Company, Minneapolis, MN). After each measurement, jars, and grids were rinsed with water and ethanol (99.8 %) and dried in an oven at 100 °C.

2.4. Device conditions and data preprocessing

2.4.1. GC-MS

Upon being securely airtight capped, these sorbents can be safely stored for a duration exceeding one week (Corion et al., 2024). In Experiment 1, the Twisters® were stored in a transport block (Gerstel) at 21 °C for a maximum of 5 days, while in Experiment 2, the storage duration was limited to 2 days before undergoing analysis using GC-MS. For the HSSE-GC-MS analysis, Twister® desorption was carried out in a thermal desorption unit (TDU) connected to a cooled injection system (CIS, Gerstel). The desorption took place with a helium flow of 50 mL/min. The TDU started at 25 °C, increased at a rate of 60 °C/min to 250 °C, and was held for 5 min. The desorbed VOCs were carried by helium into the CIS, maintained at – 50 °C. Once desorption was complete, the CIS temperature ramped at 12 °C/s to 300 °C, held for 5 min.

Chromatography was performed using an Agilent 7890A gas chromatograph coupled to an Agilent 5975C mass selective detector (Agilent Technologies, Santa Clara, CA). The GC-MS was equipped with a 30 m × 250 µm × 0.25 µm HP-5MS column (Agilent Technologies) operating at a helium flow rate of 1.07 mL/min.

The oven program consisted of an initial setpoint at 35 °C, followed by a first ramp at 4 °C/min up to 120 °C without hold time. This was succeeded by a second ramp at 6 °C/min up to 200 °C, immediately followed by a third ramp at 10 °C/min up to 250 °C, with a hold time of 5 min. The mass spectrometer scanned the range from 30 to 350 m/z, and the mass spectrometer source and mass spectrometer Quad were set at 230 °C and 150 °C, respectively.

The chromatograms and spectra were analyzed using MassHunter Workstation (Unknowns and Quantitative Analysis v10.1, Agilent Technologies). Initially, the chromatograms were subjected

to deconvolution in the Unknowns Analysis, and compounds were tentatively identified using the NIST 2020 database with a minimum match factor set at 85. The match factor evaluates the similarity between an obtained fragmentation spectrum and the theoretical fragmentation spectra of a compound in the database. The following criteria were employed to include compounds in a custom-made library: (1) a minimum match factor of 85, (2) a higher abundance in the egg measurements compared to the blank measurements, (3) a minimum occurrence of 10 % across all observations, and (4) the presence in previous in-house experiments on egg VOCs. In the second phase, these compounds underwent a double-check to ensure a realistic retention index aligned with their retention time in the chromatogram sequence. If uncertainty in compound identification arose from an unrealistic retention index or molecular mass at a specific retention time, the compound was labeled as "unknown" and maintained in the selection. Following compound selection, the Quantitative Analysis program was employed to select a quantifier ion based on its consistent and prominent signal across all observations. Simultaneously, a corresponding qualifier ion was assigned to validate the presence of the compound. Raw quantifier ion peaks exhibiting a bell curve shape underwent Gaussian smoothing, while other peaks were subjected to Savitzky-Golay smoothing. The signal of the respective compound was quantified by calculating the area under the smoothed curve.

2.4.2. PTR-TOF-MS

The PTR measurements were executed using a PTR-TOF-MS 8000 (Ionicon Analytik, Innsbruck, Austria). The bag's headspace was sampled for approximately 180 s at a flow rate of 25 mL/min through an insulated polyetheretherketone (PEEK) capillary to the drift tube of the device. The drift tube operated at 600 V, 240 Pa, and 60 °C, yielding a field density ratio (E/N) of 1.25×10^{-15} V cm² (125 Td). Inside the drift tube, analytes underwent protonation using H_3O^+ reagent ions. Subsequently, the ions were extracted every 32 µs in the time-of-flight module under a high vacuum of 8.8×10^{-5} Pa. VOCs within the range of 1 to 318 m/z were detected and averaged at intervals of 5 s. For a detailed explanation of the calibration of the spectrum mass range and the construction of the transmission curve, refer to Portillo-Estrada et al. (2021).

Subsequently, a steady signal was chosen from the individual egg spectra within the 50 to 120 s timeframe and then averaged to generate a single spectrum per egg. The spectra were cropped to a range from 15 to 318 m/z. Using the PTR-MS Viewer v3.4.4 software (Ionicon Analytik), the signal was integrated into nominal masses. Then, the raw nominal mass signal intensities were converted into adjusted product ion concentrations to remove any instrument variation by assuming the nominal masses as compounds for which concentrations were estimated (Granitto et al., 2007).

2.4.3. SIFT-MS

The SIFT-MS measurements were conducted employing a Voice200ultra instrument (Syft Technologies, Christchurch, New Zealand) with helium as the carrier gas at a flow rate of 419.71 mL/min and a tube pressure of 80.59 Pa. The headspace was sampled at a rate of 23.68 mL/min via a heated transfer line at 125 °C. Sample product ions, generated by the three reagent ions H_3O^+, NO^+, and O_2^+, were scanned over a range of 15 to 250 m/z. A sample

241 measurement comprised one preparation cycle and two sample cycles, featuring a maximum
242 scanning time of 100 ms and a count limit of 10,000 counts per m/z. The overall measurement
243 time for one sample was approximately 3.5 min. For a detailed explanation of the system validation
244 routine, refer to Corion et al. (2024). The raw signal intensities of the sample product ions were
245 expressed in count rates (cps) and were averaged for the two sample cycles. Similarly to the PTR-
246 TOF-MS data, the raw signal intensities were turned into notional analyte concentrations following
247 the approach of Benchennouf et al. (2023) to remove any instrument variation.

248 ## 2.5. Data analysis

249 The datasets were grouped per analytical technique, and subsequently split into a cross-validation
250 set and a validation set, comprising approximately 60 % and 40 % of the data, respectively. The
251 cross-validation sets were partitioned into 10 splits, ensuring equal balance in the number of
252 samples between males and females in each split. The HSSE-GC-MS datasets comprised variables
253 representing VOC peak areas, while the PTR-TOF-MS and SIFT-MS datasets featured variables
254 corresponding to product ion signals. Furthermore, the individual variables were divided by the
255 total peak area or total product ion signal to allow for a better system comparison using relative
256 abundances. Additionally, the total peak or product ion signal was included in the dataset as an
257 extra variable. Before starting the multivariate analysis, the variables were scaled to a zero mean
258 and unit variance. All datasets were analyzed by applying a partial least squares-discriminant
259 analysis (PLS-DA). The relative abundances of the VOCs or the product ions together with the
260 total peak or total product ion signal were set as predictor variables and the sex was set as a
261 categorical response variable.

262 PLS-DA models were initially constructed by utilizing the cross-validation set specific to each
263 device for each measurement day. Subsequently, these models underwent further refinement

through the application of three distinct variable selection methods: variable importance in projection (VIP), forward interval partial least squares (FiPLS), and jackknifing (JK). Concerning the VIP, each variable was considered significant if its score was 1 or higher. From the FiPLS, the number of variables was automatically chosen for a minimal root mean squared error of the cross-validation set. Finally, the JK approach was used to calculate weighted beta coefficients for variables to select those that contributed significantly to explaining the variation in the data (with $P < 0.05$). The first two variable selection methods were performed in the PLS toolbox (v8.7 2019, Eigenvector Research, Wenatchee, WA) in Matlab (v2018b, Mathworks, Natick, MA). The JK method was performed using The Unscrambler (v10.3, CAMO Software, Oslo, Norway). Finally, the models having the highest accuracy for sex prediction on the validation set were selected.

3. Results and discussion

3.1. Hatching results

Table 2 displays the hatching results obtained from the three batches. Batches 1 and 2 featured eggs of high quality, contributing 103 and 100 eggs with living embryos to the respective datasets. Batch 3 contained 33 eggs with developed embryos for analysis. Despite the loss of 10 embryos on day 12, they were included in the analysis since no aberrant data were observed from these eggs, and their sexes could be reliably determined at breakout on day 14. Plausibly, these embryos died due to the hypoxia and hypercapnia conditions induced by enclosing the eggs in a jar for 2 hours. After this 2-hour enclosure, the O_2 and CO_2 levels were 9.9 % and 9.5 %, respectively (Corion et al., 2023a). Although no embryos died on day 12 in preliminary experiments, it is conceivable that the repeated measurements of the same eggs every two days culminated in death on day 12, a point at which the stress on the embryo was at its peak due to its increased metabolic activity. In contrast, embryos from Batches 1 and 2 did not experience mortality as a result of measurements. This is likely because these eggs were measured only once, at an earlier time point (day 10), and were incubated in a recipient with double the volume. It is conceivable that these hypoxia and hypercapnia conditions affected VOC production by inducing oxidative stress within the egg, resulting in the process of lipid peroxidation into carboxylic acids (Musakhanian et al., 2022). This increase in carboxylic acids was also observed toward days 10 and 12 of incubation (Corion et al., 2023a). However, the impact on the performance of the sexing models was deemed minimal since models consistently selected the same sex-discriminating VOCs during both the early and later stages of the experiment (see later).

Table 2 – Hatching results of the three batches.

	Batch 1	Batch 2	Batch 3
Experiment	1	1	2
Analytical device	HSSE-GC-MS & PTR-TOF-MS	SIFT-MS	HSSE-GC-MS
Number of eggs	110	110	42*
Unfertilized eggs	6	10	5
Early dead embryos (< day 5)	1	0	3
Total	103	100	33†
Males	56	49	17
Females	47	51	16

*, 1 egg got lost from Batch 3; †, 9 males and 1 female died on day 12, however, they were included since no aberrant data from these eggs were observed and the sex could be well determined.

3.2. Dataset variables

A total of 117 and 162 VOCs were identified in the HSSE-GC-MS datasets of Experiments 1 and 2, respectively. Presumably, Experiment 2 identified more VOCs through extended, multiple-day samplings and the use of glass jars, which, in comparison to the less inert FEP bags, might have contributed to increasing the selection of reliably identified VOCs due to lower background noise. The identified VOCs are reported in detail in the overview tables of Appendix A. Concerning the PTR-TOF-MS and SIFT-MS data, a total of 299 and 692 product ions were included in the datasets, respectively. Despite the PTR-TOF-MS scanning across a broader mass range (15 – 318 m/z compared to 15 – 250 m/z), the SIFT-MS counted more product ions since it utilized three different reagent ions (H_3O^+, NO^+, and O_2^+) compared to only H_3O^+ for PTR-TOF-MS. For a more in-depth comparison of the three systems, reference is made to Corion et al. (2024). Finally, each dataset included the total peak signal or total product ion signal per reagent ion as a single variable. Consequently, the datasets for HSSE-GC-MS, PTR-TOF-MS, and SIFT-MS registered 118, 300, and 695 variables in Experiment 1. In Experiment 2, the HSSE-GC-MS dataset comprised a total of 163 variables.

3.3. VOC in ovo sexing on day 10 using three analytical devices

Fig. 2 presents the best-performing PLS-DA-based classification models built on the data obtained on day 10 across the three systems after variable selection. For a comprehensive overview of all prediction models developed through the three variable selection methods, refer to Supplementary Table B1 in Appendix B. Day 10 was selected since previous research indicated that VOC patterns at that day were distinct between fertilized and unfertilized eggs (Corion et al., 2023a). Hence, the expectation was that the likelihood of identifying sex-specific embryo VOCs would be high. Furthermore, Borras et al. (2023) reported the presence of sex differences in VOCs on the same day. The achieved accuracies on the validation sets ranged from 57.6 % to 61.4 %. These are significantly below the industry's prescribed target of 98 % (Fig. 2). From all models, the JK and VIP variable selection methods yielded the highest accuracies. This is in contrast to previous work on classification using egg VOCs, where the FiPLS-created models repeatedly performed better (Corion et al., 2024). One potential explanation is that when variables inherently exhibit minimal differences between response levels, selection methods such as a JK or VIP that independently assess variables may yield more robust results on validation sets compared to a FiPLS model designed to minimize the root mean squared error of the cross-validation set, thereby excluding correlated variables. The final validation on the remaining 40 % of the data revealed no substantial difference in prediction accuracy across analytical techniques, suggesting the absence of a significant correlation between the batch of eggs and the analytical device. This conclusion is underscored by the fact that Batch 1, subjected to GC-MS and PTR-TOF-MS measurements, and Batch 2, analyzed using SIFT-MS, both exhibited similar outcomes.

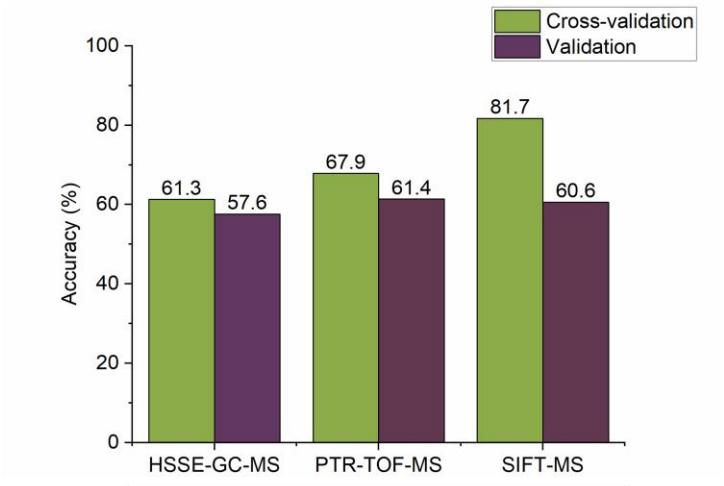

	HSSE-GC-MS	PTR-TOF-MS	SIFT-MS
$N_{Cross\text{-}validation}$	27 F / 33 M	27 F / 33 M	29 F / 31 M
$N_{Validation}$	20 F / 23 M	20 F / 23 M	22 F / 18 M
LVs	1	1	1
Variables	2	12	14
Selection method	JK	VIP	VIP

Fig. 2 – Prediction accuracies of the best-performing sex prediction models obtained after variable selection in Experiment 1. The data was acquired from VOC measurements on chicken incubation eggs on day 10 using HSSE-GC-MS, PTR-TOF-MS, and SIFT-MS. Each model was trained through cross-validation on 60 % of the data, followed by validation on the remaining 40 % of the dataset. Abbreviations: JK, Jackknifing; VIP: Variable importance in projection; LVs, Latent variables; F, Female; M, Male.

3.4. VOC in ovo sexing during the first 12 days of incubation

Building on the findings of Experiment 1, Experiment 2 was designed to optimize the VOC measurement setup by incorporating inert glass jars. The expected benefits of this setup included improved repeatability in terms of headspace volume, reduced adsorption of VOCs by the setup materials, and less risk for leaks and carryover. Furthermore, the experiment aimed to track egg VOCs across various incubation days to ascertain whether higher prediction accuracies could be achieved on days other than day 10. As the three analytical techniques did not result in different prediction accuracies, HSSE-GC-MS was selected as the preferred analytical technique, given its capability to accurately identify the measured VOCs through column separation.

Fig. 3 presents the best-performing classification models built on the data obtained throughout the first 12 days of incubation. Similarly to Experiment 1, JK and VIP yielded the highest accuracies on the validation sets. An overview of the remaining models can be found in Table B2 in Appendix B. While achieving accuracies of 90.0 % on cross-validation sets, the accuracy on validation sets varied from 63.1 % to 71.4 %, except for an accuracy of 78.6 % on day 10. However, the cross-validation accuracy on day 10 was only 70.0 %, suggesting that the higher validation set accuracy was likely a chance occurrence. Additionally, the day 10-VIP model demonstrated a more realistic accuracy of 71.4 % (refer to Table B2 in Appendix B). In general, it can be inferred that the outcomes of Experiment 2 yielded higher accuracies on the validation set when contrasted with those of Experiment 1. This can be likely attributed to the improved measurement setup, specifically the utilization of glass jars.

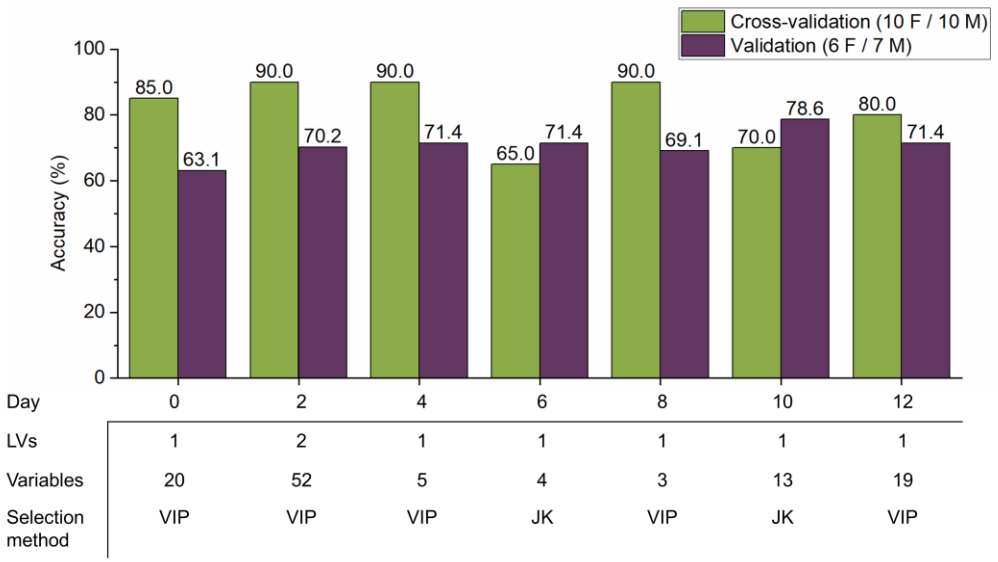

Fig. 3 – Prediction accuracies of the best-performing sex prediction models obtained after variable selection in Experiment 2. The data was acquired from VOC measurements on chicken incubation eggs on the first 12 days of incubation using HSSE-GC-MS, PTR-TOF-MS, and SIFT-MS. Each model was trained through cross-validation on approximately 60 % of the data, followed by validation on the remaining 40 % of the dataset. Abbreviations: JK, Jackknifing; VIP: Variable importance in projection; LVs, Latent variables; F, Female; M, Male.

3.5. Assessment of the Prediction Performance

In addition to evaluating validation set accuracies, the assessment of sensitivities and specificities was conducted to comprehensively appraise the predictive performance of the models. From Fig. 4 and Table B.2 in Appendix B, it was deduced that the sensitivities for females were 100 % on days 4, 6, 10, and 12. This indicates that all females in the validation set were correctly classified as females. Notably, this stands in contrast to the cross-validation set, where the predictions exhibited a more balanced distribution between the sexes. Furthermore, during both days 0 and 2, a single female was erroneously classified as male, with this misidentification consistently involving the same outlier individual on both occasions. Fig. 4 additionally illustrates that, for each daily model, multiple males were assigned a relatively high probability of being classified as females. This imbalance likely indicates that the observed number of instances was insufficient to construct robust models. Additional experiments would require an increased sample size to yield more reliable results.

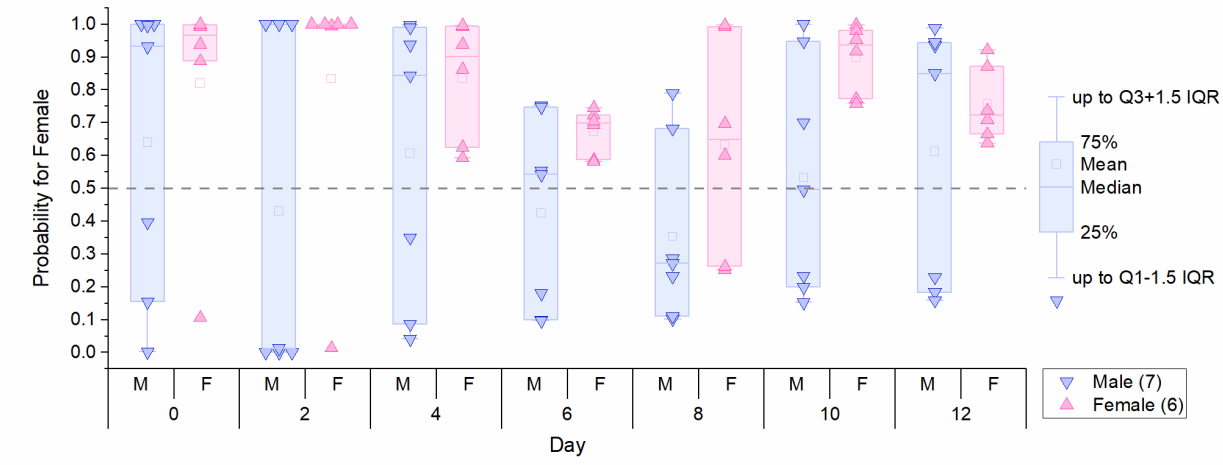

Fig. 4 – Box plot prediction probabilities of the validation data from the best-performing sex prediction models depicted in Fig. 3. A prediction threshold of 0.5 was defined, signifying that observations equal to or exceeding 0.5 were classified as female, whereas those with a probability below 0.5 were designated as male. Abbreviations: Q, Quartile; IQR, Interquartile range; M, Male; F, Female.

In a comparable study performed by Borras et al. (2023), prediction accuracies of approximately 77 % were obtained on days 8, 9, and 10. Their experiment employed active sampling at a flow rate of 50 mL/min through suction cups positioned atop the egg to cover the air sac. Twisters® were placed inside the suction cup's top wall for the VOC extraction. In one experiment, the researchers demonstrated that their predictions were better when applying active sampling versus passive sampling by incubating Twisters® inside the suction cup without providing a flow. Beyond the distinction that we enclosed the entire egg in a jar while the researchers only covered the top of the egg, three primary differences exist between our passive sampling approach and the one by Borras et al. (2023). First, we used Twisters® with a thicker polydimethylsiloxane (PDMS) coating, providing more sorbent material (1 mm vs. 0.5 mm). Second, we applied a 2-hour extraction vs. 15 minutes. And third, we made use of glass material vs. the translucent silicone of the suction cups.

Our methodology is motivated by the fact that this setup resulted in the highest number of well-identified VOCs in preliminary experiments. Concerning the extraction time, Twisters® captured fewer VOCs at shorter extraction times and also longer extraction times negatively affected Twister® performance (results not presented). We attributed the decline in performance at longer extraction times to the rising moisture levels within the jar, as it is well-established that humid conditions negatively affect VOC adsorption (Maceira et al., 2017). Furthermore, we used inert glass to minimize adsorption competition with the Twisters®. Concerning the suction cups, there is a potential interference with VOC adsorption due to the use of silicone materials, typically made from PDMS (Femmer et al., 2015), wich is also the same material of the Twisters®. Therefore, we cannot compare our setup 1-on-1 with the setup of Borras et al. Nevertheless, it is noteworthy that the researchers achieved higher prediction accuracies with active sampling (77 % as opposed to

411 our 71.4 %). Hence, it would be interesting in the future to further explore the active sampling
412 approach using thicker PDMS coatings of 1 mm and more inert materials for the suction cups such
413 as Teflon®. Other advantages of active sampling would be the fact that these can be performed in
414 an open system and this will avoid hypercapnia and hypoxia conditions that might perturbate
415 normal metabolic conditions of the embryos (Borras et al., 2023).

416 3.6. Identification of consistently discriminatory compounds

417 In Fig. 5, we present the abundances per day of variables that appeared four or more times in the
418 best-performing prediction models from Fig. 3. These variables corresponded to the relative
419 abundances of furan-2-carbaldehyde, phenol, and tetradecanal. Additionally, the total peak signal
420 was consistently included in five of the best-performing daily models. A fifth variable emerged as
421 a selected compound in four models. However, its specific identity remained unknown, and it was
422 named as Unknown IV. Notably, the abundances of the respective compounds were consistent
423 over time. To elaborate, furan-2-carbaldehyde, phenol, and Unknown IV consistently
424 demonstrated higher levels in females, while tetradecanal and the total peak signal exhibited higher
425 abundances in males. Furthermore, it was observed that all four VOCs and the total VOC
426 abundance decreased towards later incubation days. This pattern of decreasing egg VOCs was
427 highlighted in a previous study (Corion et al., 2023a), which noted the general decline throughout
428 the incubation of fertilized eggs. One plausible hypothesis posited that since VOCs typically derive
429 from amino acids, fatty acids, and carotenoids, these compounds undergo conversion during both
430 egg deterioration and embryonic development. For example, approximately 50 % of the total yolk
431 fatty acids are metabolized for energy, while the remaining 50 % will be converted into body
432 tissues and residual yolk of the newly hatched chicken (Lin et al., 1991). Consequently, the
433 presence of these compounds diminishes, leading to a reduced capacity for generating new VOCs.

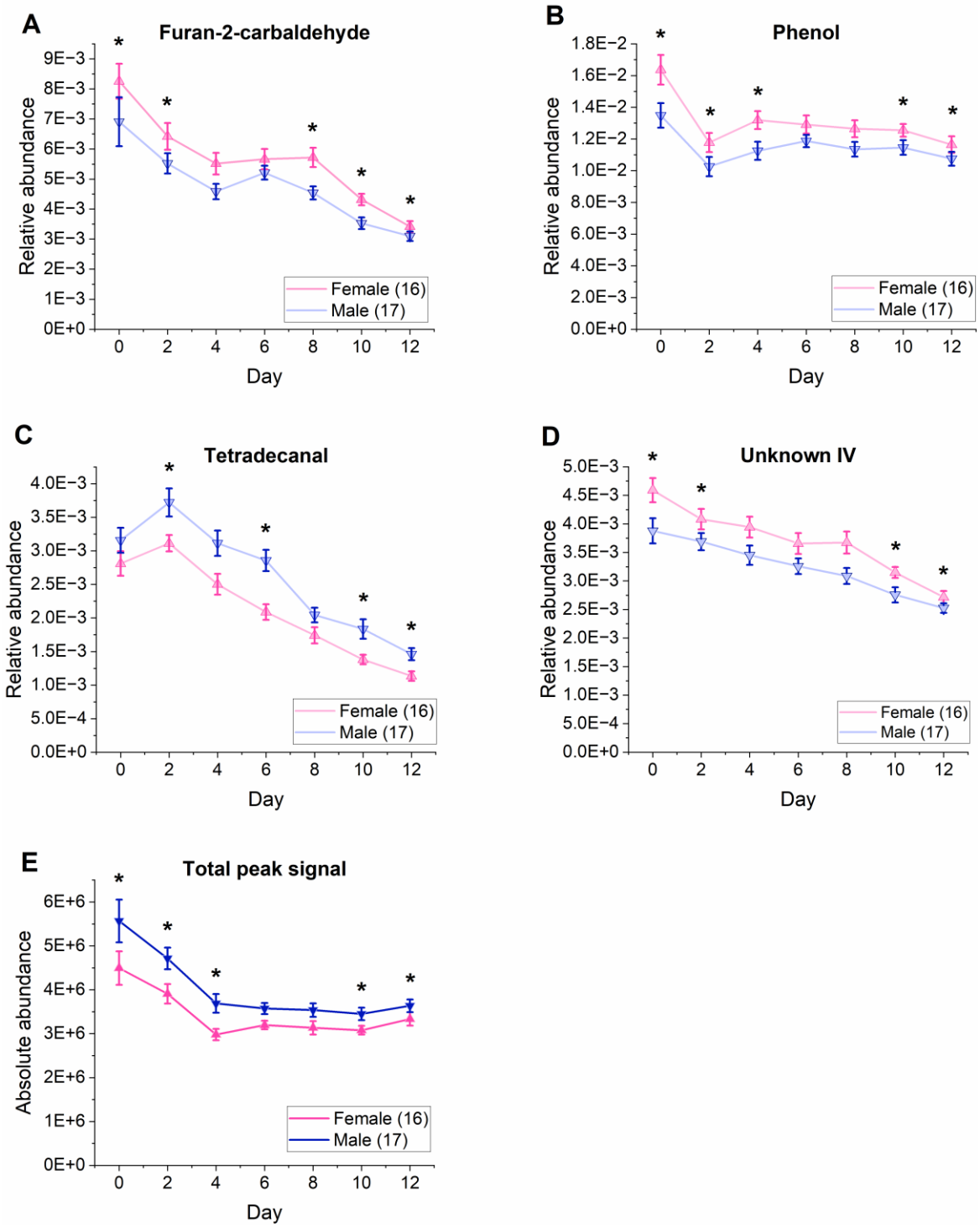

Fig. 5 – Average abundances of variables that were included four or more times in the best-performing sex prediction models from Fig. 3. The asterisk indicates the days on which the variable was included in the model and the error bar represents the standard error on the mean. Relative abundances over time of (A) Furan-2-carbaldehyde, (B) Phenol, (C) Unknown IV, and (D) Tetradecanal. (E) Absolute abundance of the total peak signal over time.

Furan-2-carbaldehyde, also known as furfural, can originate as a product of the Maillard reaction from the amino acid serine and the sugars glucose and fructose, as illustrated in the case of sugarcane juice (Huang et al., 2023). Serine is known to be present in egg white and yolk proteins (Belitz et al., 2009). Whereas glucose is the most dominant sugar present in egg carbohydrates, particularly in the egg white (Réhault-Godbert et al., 2019). While it is not known whether furfural is naturally produced by plants or animals, it is plausible that furfural emissions may arise from the breakdown of compounds such as serine or glucose.

Similar to our findings, phenol was earlier found to be significantly higher in quail eggs containing female embryos (Webster et al., 2015). Phenol can be a direct product of the amino acid L-tyrosine (Antson et al., 1993). Physiologically, tyrosine metabolism is known to be influenced by estradiol concentrations (Presch and Lubec, 1994) and tyrosine itself is also known as a precursor for melanin synthesis (Li et al., 2019). Both estradiol and melanin are known to differ between the sexes (Weissmann et al., 2013; Corion et al., 2022). Plasma 17B-estradiol levels differ significantly between the sexes after 7.5 incubation days (Woods and Brazzill, 1981), while differences in melanin pigmentation in breeds with sex-specific coloring start to occur on incubation day 12 (Corion et al., 2022). Hypothetically, these sex-specific differences might impact tyrosine utilization in the chicken embryo, potentially contributing to differences in phenol emissions.

Tetradecanal was generally higher in relative abundance in male eggs. Aldehydes, including tetradecanal, are recognized to originate from fatty and amino acids, and they can undergo subsequent reduction by alcohol dehydrogenases to form the corresponding alcohols (Belitz et al., 2009). Furthermore, Hiremath et al. (1992) demonstrated that the activity of alcohol dehydrogenase can undergo a notable increase, ranging from 5 to 7-fold, following estradiol

treatment. Consequently, it is hypothesized that aldehyde reduction through alcohol dehydrogenases might occur at a higher rate in female embryos due to the higher estradiol levels. This could lead to higher levels of aldehydes such as tetradecanal in males. Similarly, higher relative and absolute abundance levels were found in males in un-, do-, tri-, penta-, and hexadecanal as well throughout the incubation period (results not presented). Finally, the total peak abundance was higher in eggs containing male embryos. This implies that males generally emitted higher abundances of VOCs throughout incubation. Unlike prior studies showing higher VOC levels in female chicken, quail, and barn swallow eggs (Webster et al., 2015; Costanzo et al., 2016; Xiang et al., 2022), our study revealed contrasting results. However, no clear explanation was found for these differences.

It is important to mention that the prediction models were built on the relative abundances of VOCs and that the relative levels of the selected variables therefore also depended on the abundances of other compounds. Furan-2-carbaldehyde and phenol were for instance not significantly different between the sexes in their absolute abundance. In contrast, tetradecanal exhibited significantly higher absolute abundances among males, aligning with its relative prevalence. To ensure the VOC sexing models' robustness, it is crucial to identify those VOCs that consistently demonstrate discriminatory characteristics. In our study, we identified VOCs that exhibited consistent levels throughout the incubation period. Future experiments should aim to validate this observed consistency and identify specific VOCs that are consistently discriminating on specific days. Additionally, unraveling the underlying mechanisms will not only enhance our understanding of the physiological background but also strengthen the model's credibility.

4. Conclusion

Following our primary aim to assess the viability of VOC in ovo sexing using three different analytical devices, no significant differences were found on day 10 between the standard HSSE-GC-MS and the faster acquisition techniques, namely PTR-TOF-MS and SIFT-MS. The accuracies ranging from 57.6 % to 61.4 % demonstrated a substantial underperformance compared to the industry's benchmark of 98 %. Possibly, the background noise of the sampling bags negatively affected the analysis. Consequently, we optimized the sampling setup using more inert glass jars and exclusively relied on HSSE-GC-MS for analysis to enhance sex prediction accuracy and identify relevant VOCs during the initial 12 days of incubation. As a result, higher accuracies were obtained ranging from 63.1 % to 71.4 %. Furthermore, we suggested the need for more data to improve model robustness. Particularly, imbalances in prediction performance were observed, resulting in a 100 % correct classification of females on days 4, 6, 10, and 12. Another suggestion for improving prediction performance involved investigating active sampling through suction cups constructed from inert material. Finally, furan-2-carbaldehyde, phenol, and tetradecanal emerged as VOCs consistently exhibiting elevated relative abundances specific to a particular sex, with the overall VOC abundance averaging higher in male embryos. Investigating the intrinsic mechanisms behind these VOC emissions would not only advance our comprehension of the physiological context but also enrich and reinforce the efficacy of in ovo sexing prediction models based on VOCs.

ACKNOWLEDGMENTS

Gratitude is expressed to Elfie Dekempeneer for her support in operating the GC-MS device. This work has received funding from the Flemish Environment Department, the Foundation for Food and Agricultural Research [EggTech-0000000028], and the Research Foundation – Flanders [M.C. was funded by an SB project 1SC7219N and S.S. was funded by an SB project 1S54823N].

DECLARATION OF INTEREST

All the authors declare that they have no conflict of interest.

DECLARATION OF GENERATIVE AI AND AI-ASSISTED TECHNOLOGIES IN THE WRITING PROCESS

During the preparation of this work, the authors used Chat-GPT in order to improve the manuscript's readability. After using this tool, the authors reviewed and edited the content as needed and take full responsibility for the content of the publication.

REFERENCES

Antson, A. A., T. V. Demidkina, P. Gollnick, Z. Dauter, R. L. Von Tersch, J. Long, S. N. Berezhnoy, R. S. Phillips, E. H. Harutyunyan, and K. S. Wilson. 1993. Three-dimensional structure of tyrosine phenol-lyase. Biochemistry 32:4195–4206 Available at https://pubs.acs.org/doi/abs/10.1021/bi00067a006.

Belitz, H.-D., W. Grosch, and P. Schieberle. 2009. Food Chemistry. 4th revise. Springer Berlin Heidelberg, Berlin, Heidelberg.

Benchennouf, A., M. Corion, A. Dizon, Y. Zhao, J. Lammertyn, B. De Coninck, B. Nicolaï, J. Vercammen, and M. Hertog. 2023. Increasing the Robustness of SIFT-MS Volatilome Fingerprinting by Introducing Notional Analyte Concentrations. J. Am. Soc. Mass Spectrom. 34:2407–2412 Available at https://pubs.acs.org/doi/10.1021/jasms.3c00168.

Borras, E., Y. Wang, P. Shah, K. Bellido, K. L. Hamera, R. A. Arlen, M. M. McCartney, K. Portillo, H. Zhou, C. E. Davis, and T. H. Turpen. 2023. Active sampling of volatile chemicals for non-invasive classification of chicken eggs by sex early in incubation (FYH Kutsanedzie, Ed.). PLoS One 18:e0285726 Available at http://dx.doi.org/10.1371/journal.pone.0285726.

Bruijnis, M. R. N., V. Blok, E. N. Stassen, and H. G. J. Gremmen. 2015. Moral “Lock-In” in Responsible Innovation: The Ethical and Social Aspects of Killing Day-Old Chicks and Its Alternatives. J. Agric. Environ. Ethics 28:939–960.

Bruins, W. S., and W. M. Stutterheim. 2017. Method and system for the non-destructive in ovo determination of fowl gender. Available at https://worldwide.espacenet.com/patent/search/family/059366469/publication/WO2017204

636A2?q=pn%3DWO2017204636A2&queryLang=en%3Ade%3Afr.

Bundestag. 2019. Deutscher Bundestag, Gesetzentwurf der Bundesregierung. :176 Available at https://dip21.bundestag.de/dip21/btd/19/134/1913452.pdf.

Busse, M., M. L. Kernecker, J. Zscheischler, F. Zoll, and R. Siebert. 2019. Ethical Concerns in Poultry Production: A German Consumer Survey About Dual Purpose Chickens. J. Agric. Environ. Ethics 32:905–925 Available at https://doi.org/10.1007/s10806-019-09806-y.

Corion, M., J. Keresztes, B. De Ketelaere, and W. Saeys. 2022. In ovo sexing of eggs from brown breeds with a gender-specific color using visible-near-infrared spectroscopy: effect of incubation day and measurement configuration. Poult. Sci. 101:101782 Available at https://doi.org/10.1016/j.psj.2022.101782.

Corion, M., M. Portillo-Estrada, S. Santos, J. Lammertyn, B. De Ketelaere, and M. Hertog. 2024. Non-destructive egg breed separation using advanced VOC analytical techniques HSSE-GC-MS, PTR-TOF-MS, and SIFT-MS: Assessment of performance and systems' complementarity. Food Res. Int. 176:113802 Available at https://doi.org/10.1016/j.foodres.2023.113802.

Corion, M., S. Santos, N. Everaert, J. Lammertyn, and B. De Ketelaere. 2023a. Non-Invasive Assessment of Chicken Egg Fertility during Incubation using HSSE-GC-MS VOC Profiling. ChemRxiv:1–33 Available at https://doi.org/10.26434/chemrxiv-2023-q609g.

Corion, M., S. Santos, B. De Ketelaere, D. Spasic, M. Hertog, and J. Lammertyn. 2023b. Trends in in ovo sexing technologies: insights and interpretation from papers and patents. J. Anim. Sci. Biotechnol. 14:102 Available at https://doi.org/10.1186/s40104-023-00898-1.

560 Costanzo, A., S. Panseri, A. Giorgi, A. Romano, M. Caprioli, and N. Saino. 2016. The Odour of
561 Sex: Sex-Related Differences in Volatile Compound Composition among Barn Swallow Eggs
562 Carrying Embryos of Either Sex (JM Avilés, Ed.). PLoS One 11:e0165055 Available at
563 https://dx.plos.org/10.1371/journal.pone.0165055.

564 Drouin, N., H. L. Elfrink, W. Bruins, S. Koval, A. C. Harms, W. Stutterheim, and T. Hankemeier.
565 2023. How to prevent chick culling in the poultry industry ? Discovery of a new biomarker
566 for in ovo gender screening. BioRxiv Available at
567 https://doi.org/10.1101/2023.08.20.551526.

568 Einspanier, A. 2017. Method for the in-ovo sex identification of chicks.

569 Femmer, T., A. J. C. Kuehne, J. Torres-Rendon, A. Walther, and M. Wessling. 2015. Print your
570 membrane: Rapid prototyping of complex 3D-PDMS membranes via a sacrificial resist. J.
571 Memb. Sci. 478:12–18 Available at
572 https://linkinghub.elsevier.com/retrieve/pii/S0376738814009430.

573 Gabbai, E. 2019. A system and method for non-invasively determining egg properties. Available
574 at https://worldwide.espacenet.com/patent/search?q=pn%3DWO2019021275A1.

575 Giersberg, M., and N. Kemper. 2018. Rearing Male Layer Chickens: A German Perspective.
576 Agriculture 8:176 Available at https://doi.org/10.3390/agriculture8110176.

577 Governo Italiano. 2023. Communicato stampa del consiglio dei ministri n.49. Available at
578 https://www.governo.it/it/articolo/comunicato-stampa-del-consiglio-dei-ministri-n-
579 49/23491 (verified 27 December 2023).

580 Granitto, P., F. Biasoli, E. Aprea, D. Mott, C. Furlanello, T. Mark, and F. Gasperi. 2007. Rapid

and non-destructive identification of strawberry cultivars by direct PTR-MS headspace analysis and data mining techniques. Sensors Actuators B Chem. 121:379–385 Available at https://linkinghub.elsevier.com/retrieve/pii/S0925400506002577.

Haase, A., B. M. Schusser, M. Molina-Romero, P. A. Goméz, M. Aigner, S. Huber, and A. Joos. 2019. Automated noninvasive determining the sex of an embryo and the fertility of a brid's egg. Available at https://worldwide.espacenet.com/patent/search?q=pn%3DWO2019092265A1.

HIREMATH, L. S., P. M. KESSLER, G. C. SASAKI, and P. E. KOLATTUKUDY. 1992. Estrogen induction of alcohol dehydrogenase in the uropygial gland of mallard ducks. Eur. J. Biochem. 203:449–457 Available at https://febs.onlinelibrary.wiley.com/doi/10.1111/j.1432-1033.1992.tb16569.x.

Huang, H., J. Chen, M. Zheng, L. Zhang, H. Ji, H. Cao, F. Dai, and L. Wang. 2023. Precursors and formation pathways of furfural in sugarcane juice during thermal treatment. Food Chem. 402:134318 Available at https://doi.org/10.1016/j.foodchem.2022.134318.

Knepper, P., M. O'Hayer, and J. Hoopes. 2018. System and method for in ovo sexing of avian embryos. :33 Available at https://worldwide.espacenet.com/patent/search?q=pn%3DWO2018023105A1.

Kollmansperger, S., M. Anders, J. Werner, A. M. Saller, L. Weiss, S. C. Süß, J. Reiser, G. Schneider, B. Schusser, C. Baumgartner, and T. Fenzl. 2023. Nociception in Chicken Embryos, Part II: Embryonal Development of Electroencephalic Neuronal Activity In Ovo as a Prerequisite for Nociception. Animals 13:2839 Available at https://www.mdpi.com/2076-2615/13/18/2839.

603 Krautwald-Junghanns, M. E., K. Cramer, B. Fischer, A. Förster, R. Galli, F. Kremer, E. U. Mapesa,
604 S. Meissner, R. Preisinger, G. Preusse, C. Schnabel, G. Steiner, and T. Bartels. 2018. Current
605 approaches to avoid the culling of day-old male chicks in the layer industry, with special
606 reference to spectroscopic methods. Poult. Sci. 97:749–757.

607 Li, D., X. Wang, Y. Fu, C. Zhang, Y. Cao, J. Wang, Y. Zhang, Y. Li, Y. Chen, Z. Li, W. Li, R.
608 Jiang, G. Sun, Y. Tian, G. Li, and X. Kang. 2019. Transcriptome Analysis of the Breast
609 Muscle of Xichuan Black-Bone Chickens Under Tyrosine Supplementation Revealed the
610 Mechanism of Tyrosine-Induced Melanin Deposition. Front. Genet. 10:1–13 Available at
611 https://www.frontiersin.org/article/10.3389/fgene.2019.00457/full.

612 Lin, D. S., W. E. Connor, and G. J. Anderson. 1991. The Incorporation of n-3 and n-6 Essential
613 Fatty Acids into the Chick Embryo from Egg Yolks Having Vastly Different Fatty Acid
614 Compositions. Pediatr. Res. 29:601–605 Available at
615 https://www.nature.com/doifinder/10.1203/00006450-199106010-00015.

616 Maceira, A., L. Vallecillos, F. Borrull, and R. M. Marcé. 2017. New approach to resolve the
617 humidity problem in VOC determination in outdoor air samples using solid adsorbent tubes
618 followed by TD-GC–MS. Sci. Total Environ. 599–600:1718–1727 Available at
619 http://dx.doi.org/10.1016/j.scitotenv.2017.05.141.

620 McKay, J. C. 2014. Spectrophotometric analysis of embryonic chick feather color. Available at
621 https://worldwide.espacenet.com/patent/search?q=pn%3DUS2014069336A1.

622 Musakhanian, J., J.-D. Rodier, and M. Dave. 2022. Oxidative Stability in Lipid Formulations: a
623 Review of the Mechanisms, Drivers, and Inhibitors of Oxidation. AAPS PharmSciTech
624 23:151 Available at https://doi.org/10.1208/s12249-022-02282-0.

625 Portillo-Estrada, M., C. Van Moorleghem, S. Janssenswillen, R. J. Cooper, C. Birkemeyer, K.
626 Roelants, and R. Van Damme. 2021. Proton-transfer-reaction time-of-flight mass
627 spectrometry (PTR-TOF-MS) as a tool for studying animal volatile organic compound (VOC)
628 emissions (P Durand, Ed.). Methods Ecol. Evol. 12:748–766 Available at
629 https://onlinelibrary.wiley.com/doi/10.1111/2041-210X.13554.

630 Presch, I., and G. Lubec. 1994. The effect of ovariectomy on phenylalanine and tyrosine
631 metabolism. Amino Acids 7:57–66 Available at
632 http://link.springer.com/10.1007/BF00808446.

633 Réhault-Godbert, S., N. Guyot, and Y. Nys. 2019. The Golden Egg: Nutritional Value,
634 Bioactivities, and Emerging Benefits for Human Health. Nutrients 11:684 Available at
635 https://www.mdpi.com/2072-6643/11/3/684.

636 Reithmayer, C., M. Danne, and O. Mußhoff. 2021. Look at that!—The effect pictures have on
637 consumer preferences for in ovo gender determination as an alternative to culling male chicks.
638 Poult. Sci. 100:643–653 Available at
639 https://linkinghub.elsevier.com/retrieve/pii/S0032579120307744.

640 République Française. 2022. Journal officiel - lois et décerets. Available at
641 https://www.legifrance.gouv.fr/jorf/jo/2022/02/06/0031 (verified 9 May 2023).

642 Rivers, A. R. 2021. System and method for determining the sex and viability of poultry eggs prior
643 to hatching. Available at
644 https://worldwide.espacenet.com/patent/search?q=pn%3DUS2021181174A1.

645 Tongli, S., X. Lin, and Y. Xiaohai. 2019. The invention discloses a terahertz poultry embryo sex
646 detection device. Available at

https://worldwide.espacenet.com/patent/search?q=pn%3DCN208891459U.

Webster, B., W. Hayes, and T. W. Pike. 2015. Avian Egg Odour Encodes Information on Embryo Sex, Fertility and Development (N Saino, Ed.). PLoS One 10:e0116345 Available at https://dx.plos.org/10.1371/journal.pone.0116345.

Weigel, M. C., K. Hofmann-Peiker, and M. Kleine. 2017. Method for gender identification in domestic chicken. Available at https://worldwide.espacenet.com/patent/search?q=pn%3DWO2017076957A1.

Weissmann, A., S. Reitemeier, A. Hahn, J. Gottschalk, and A. Einspanier. 2013. Sexing domestic chicken before hatch: A new method for in ovo gender identification. Theriogenology 80:199–205 Available at http://dx.doi.org/10.1016/j.theriogenology.2013.04.014.

Woods, J. E., and D. M. Brazzill. 1981. Plasma 17β-estradiol levels in the chick embryo. Gen. Comp. Endocrinol. 44:37–43 Available at https://linkinghub.elsevier.com/retrieve/pii/0016648081903531.

Xiang, X., G. Hu, Y. Jin, G. Jin, and M. Ma. 2022. Nondestructive characterization gender of chicken eggs by odor using SPME/GC-MS coupled with chemometrics. Poult. Sci. 101:101619 Available at https://doi.org/10.1016/j.psj.2021.101619.